Design of a Slotless Structure for Minimizing Cogging Torque and Torque Ripple in a Column Type EPS Motor for Vehicles

Do-Hyeon Choi[1], Dong-Ho Kim[2], Hyung-Sub Han[1], Dong-Hoon Jung[3], and Won-Ho Kim[4]

[1]Department of Next Generation Smart Energy System Convergence, Gachon University, Seongnam 13120, Republic of Korea
[2]Department of Electrical Engineering, Hanyang University, Seoul 04763, Republic of Korea
[3]Department of Electrical and Materials Engineering, Andong National University, Andong 36729, Republic of Korea
[4]Department of Electrical Engineering, Gachon University, Seongnam 13120, Republic of Korea

Currently, the automotive market is undergoing a vibrant transition toward component electrification driven by the widespread adoption of electric vehicles. The steering system, electric power steering (EPS), has evolved gradually from traditional hydraulic systems (HPSs) to electric systems. The current state sees the majority of commercial vehicles equipped with electric EPS systems. EPS reduces the steering effort applied to the steering wheel during low-speed driving, enhancing driving convenience. It is widely adopted in most commercial vehicles due to numerous advantages such as system simplification, speed-dependent steering control, and vehicle weight reduction compared to traditional HPSs. EPS can achieve a 3%–5% improvement in fuel efficiency compared to traditional HPSs because it operates only when the driver manipulates the steering wheel. However, what matters most in EPS is vibration and noise. Drivers are directly exposed to the vibration and noise of EPS. Therefore, it is crucial to implement electromagnetic designs that reduce cogging torque and torque ripple, which are the causes of vibrations and noise in electric motors. However, due to the inherent characteristics of electric motors, in structures designed for winding coil windings, such as fixed stator slots and teeth, the variation in reluctance during operation is not consistent. Consequently, this leads to an increase in the occurrence of cogging torque and torque ripple. However, if an EPS motor is designed with a structure lacking stator teeth, the change in reluctance during rotor rotation remains constant. In theory, this would significantly reduce cogging torque and torque ripple when the rotor is in motion. Therefore, in this article, the conventional EPS motor, designed with a structure containing stator teeth resulting in cogging torque and torque ripple, is targeted for reduction. This article designed a slotless motor structure with the goal of significantly minimizing these effects. In this article, pursued a design to achieve the target output of the EPS slotless motor and enhance the overall output density. Ultimately, this motor designed, fabricated, and analyzed a motor for the automotive EPS system with the capability to reduce vibrations and noise while achieving weight reduction.

Index Terms— **Cogging torque, column type, electric power steering (EPS), slotless, torque ripple.**

I. Introduction

THIS article proposes a new concept of a slotless motor that can significantly reduce vibration and noise. Therefore, research aimed at reducing the primary causes of motor vibration and noise, namely cogging torque and torque ripple, is crucial. In motors, cogging torque and torque ripple primarily occur due to the presence of slots in the stator structure. The slotted structure designed for winding coils creates differences in reluctance, leading to the generation of cogging torque and torque ripple. Changing the stator teeth is one method to reduce cogging torque [1]. Another approach involves altering the shape of the rotor instead of the stator [2]. Alternatively, skewing can be applied to the core to mitigate these issues [3]. There are also studies exploring unconventional spherical shapes for motors, differing from conventional designs [4]. However, these methods may not yield a significant reduction. A motor capable of addressing such challenges is the slotless motor. However, conventional slotless motors encounter difficulties in securing the coil, making manufacturing complex. This issue has been tackled by designing a new combination of blocks and coils. In addition, by leveraging the high BH_{max} characteristics of permanent magnets in slotless motor, output can be maximized. Through the slotless structure, spatial constraints can be met, enabling compactness and increasing gravimetric power density. In addition, the novel block-structured slotless motor effectively eliminates major radial forces with very low cogging torque, thereby minimizing total harmonic distortion (THD) and ultimately implementing a low-noise motor by greatly reducing torque ripple, a root cause of vibration and noise. Through this slotless block structure, high output is achieved, compactness is attained to increase power density, and a significant reduction of electromagnetic vibration and noise, primarily caused by cogging torque and torque ripple, is achieved, thereby mitigating vibration and noise. Finally, compared to conventional electric power steering (EPS) motors, downsizing and creating a low-noise motor were validated through the design, manufacturing, and testing of prototypes via electromagnetic and mechanical design. In conclusion, by combining the use of high BH_{max} permanent magnets and slotless block structure, this motor satisfies quantitative objectives that were limitations of conventional EPS motors and overcomes the constraints of existing technologies.

Research on slotless motors is currently receiving considerable attention in the field of motor studies. There has

Manuscript received 23 March 2024; revised 27 June 2024; accepted 10 July 2024. Date of publication 17 July 2024; date of current version 27 August 2024. Corresponding author: W.-H. Kim (e-mail: wh15@gachon.ac.kr).

Color versions of one or more figures in this article are available at https://doi.org/10.1109/TMAG.2024.3428343.

Digital Object Identifier 10.1109/TMAG.2024.3428343

been a surge in research on slotless motors in recent years. Various types of slotless motors are being actively investigated, including those employing methods such as winding coils [5], toroidal slotless motors [6], [7], axial slotless motors [8], and analyses of vibration in slotless motors [9]. In conventional motors with slots, the stator teeth are known to cause unevenness in reluctance. This unevenness in reluctance leads to the generation of cogging torque and torque ripple, which are the root causes of vibration and noise. However, slotless motors offer a significant advantage as the difference in reluctance remains uniform during rotor rotation, resulting in very low levels of cogging torque and torque ripple. To eliminate the slots in the stator, consideration must be given to a structure that securely fixes the coils. In addition, the increase in the number of winding layers affects the magnetic airgap, thereby influencing the output. Thus, design considerations should include voltage limitations. Slotless motors offer the advantage of being able to utilize a greater amount of permanent magnets due to the absence of stator teeth magnetic saturation. To meet output requirements and reduce the weight of the motor, optimal design regarding the use of permanent magnets and the number of winding turns is crucial. Therefore, this article proposes a design process for the C-Type EPS slotless motor that aligns with these considerations.

II. EPS Slotless Motor

Fig. 1 shows the design process of the C-Type EPS slotless motor. First, the necessary specifications are determined during the design phase. The motor is specified as a 12 V C-Type EPS motor with a rated operating speed of 1000 rpm. Once the required specifications are established, the overall size of the motor is determined. As previously described, in slotless motors, winding design is crucial. The diameter of the coil and the number of layers affect the magnetic air gap length. The number of layers of the coil and the thickness of the permanent magnets are determined to comply with the voltage usage restrictions. Slotless motor feature a simple stator yoke shape resembling a ring, without the presence of stator teeth. Due to the low magnetic saturation of the iron core, the back electromotive force (BEMF) exhibits linear behavior. Moreover, with minimal magnetic saturation, slotless motors can utilize a greater amount of permanent magnets. However, the magnetic flux of permanent magnets exhibits a linear increase in BEMF with usage until a turning point, after which it decreases nonlinearly. The amount of permanent magnet usage is determined by comparing the magnetic flux density at the air gap. Then, the determination of coil layers and turns is made to meet the target specifications, followed by the determination of the current vector.

Fig. 2(a) shows diagrams of the conventional model and the slotless model, while (b) shows the designation of the Slotless EPS Motor components. Due to the absence of stator teeth in slotless motor, a significant amount of magnetic flux from the permanent magnets can be utilized. Consequently, it allows for the design of reducing the overall weight while increasing the gravimetric power density at the same output level. In addition, due to the uniform variation in reluctance, the cogging torque, which is the force attempting to align the rotor's permanent

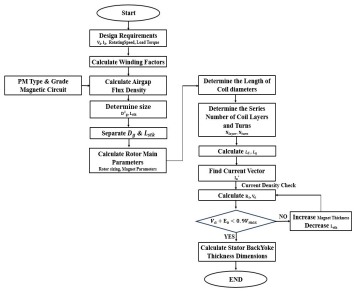

Fig. 1. C-Type EPS slotless motor process.

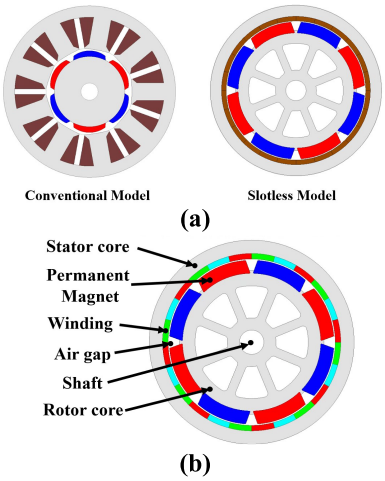

Fig. 2. (a) Diagram of conventional and slotless model. (b) Terminology of the slotless motor.

magnets with the stator's iron core, is greatly reduced. Such slotless motors exhibit minimal cogging torque, leading to the elimination of radial forces in the motor and, consequently, reducing THD and mitigating torque ripple, which affects vibration and noise.

Fig. 3 shows the 3-D model and actual prototype model of the C-Type EPS Slotless Motor. Fig. 3(a) is the rotor 3-D model and fabricated rotor, (b) is the block and coil winding 3-D model and fabricated block coil, and (c) is the full 3-D model shape. The rotor consists of a surface-mounted permanent magnet synchronous motor (SPMSM), where permanent magnets are attached to the outer surface of the rotor core. The stator is composed of block and coil, where blocks are injected over the coils, and an outer ring-shaped stator backyoke is fit. In contrast to conventional motors where coils are wound around teeth on the stator core, typical slotless motors are solely coil wound. However, winding coils alone pose challenges in manufacturing and are disadvantageous for mass production. Conversely, the block and coil winding method, which involves injecting blocks into coils, offers superior manufacturability and is conducive to mass production. In addition, it provides a stable assembly structure for coils, ensuring stability. Such a stable structure helps reduce motor vibration and noise.

Table I shows the specifications of the design model. Permanent magnets with increased B_r values were used to match the final model, the block and coil slotless motor. In conventional models, it is challenging to use permanent magnets with such high B_r values due to considerations of stator teeth saturation.

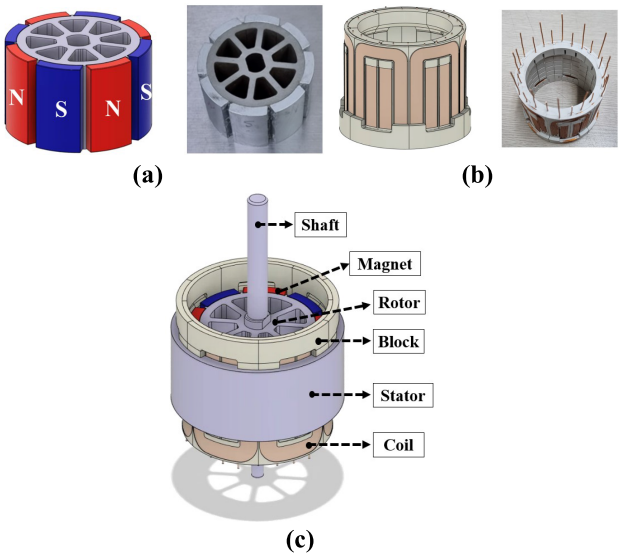

Fig. 3. (a) Rotor 3-D model and fabricated rotor. (b) Block and coil winding 3-D model and fabricated block and coil winding. (c) Slotless motor 3-D final model.

TABLE I
DESIGN SPECIFICATIONS FOR C-TYPE EPS SLOTLESS MOTOR

PARAMETER	VALUE	UNIT
Pole / Slot	8 / 24	-
Stator Diameter	84	mm
Rotor Diameter	67.5	mm
Airgap length	0.5	mm
Stack length	38.5	mm
Coil diameter (full size)	0.8(0.85)	mm
Coil Turns	17	-
Parallel Number	4	-
Magnet	1.43/1109	T/ (ka/m)
Coil	Copper	-
Core	50PN470	-

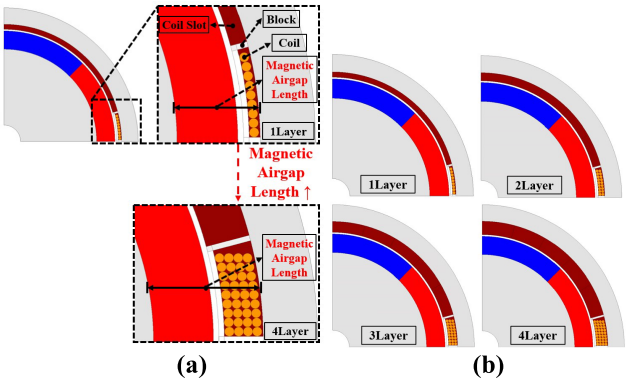

Fig. 4. (a) Increase in magnetic airgap length with increase in number of coil layers. (b) Changes with increasing number of coil layers.

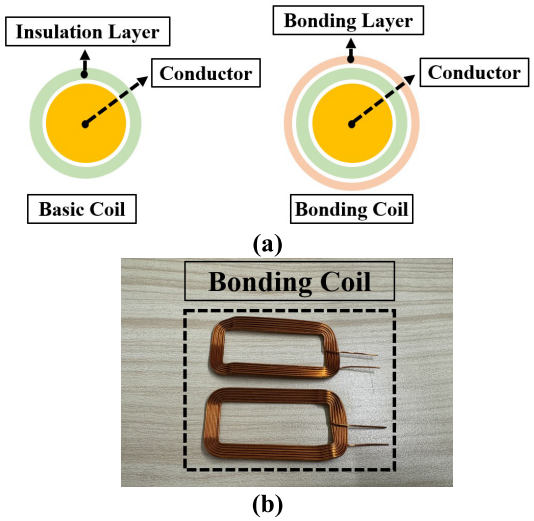

Fig. 5. (a) Basic coil and bonding coil. (b) Fabricated bonding coil.

However, slotless motors offer the advantage of using high B_r value permanent magnets and increasing the amount of magnet usage to reduce motor weight. Bonding coils coated with a bonding layer were utilized for the coil.

Fig. 4 shows the diagram concerning the most critical aspect of coil design, the number of coil layers. First, (a) shows how the magnetic airgap increases with the number of coil layers. From a magnetic perspective, both the coil and permanent magnet have a permeability similar to that of air, resulting in an increase in the magnetic airgap. Fig. 4(b) shows the variations in shape corresponding to the number of coil layers in a 2-D section. Such increases in the thickness of magnets or the number of coil layers may lead to an increase in the magnetic airgap, which could cause a decrease in output. This effect can be likened to an increase in the physical airgap. Consequently, this consideration guides the design of both permanent magnets and coils.

Fig. 5(a) shows a section comparing a basic coil with a bonding coil. The bonding coil is formed by adding a bonding layer on top of a basic coil, followed by applying heat to maintain its shape. In conventional slotless motor, there is an issue of coils coming loose due to the absence of a supporting structure. These bonding coils can address the drawbacks of the conventional slotless motor manufacturing method.

III. C-TYPE EPS SLOTLESS MOTOR FEA DATA

Fig. 6(a) shows the flux lines of the slotless model, while (b) is the magnetic equivalent circuit. In the magnetic equivalent circuit, the permanent magnet flux is represented as $\Phi_r/2$, indicating that half of the flux flows in the opposite direction, as shown in (a). The reluctance components are denoted by R for each material. In motors with slots, the flux follows the teeth of the stator, so only airgap reluctance affects the magnetic flux. However, in slotless motors, the reluctance of the coil also affects the magnetic flux since there are no stator teeth. This shows an increase in the length of the magnetic airgap.

Fig. 7 shows the comparison of noload back EMF with respect to the number of poles and coil layers. The selection of poles is crucial for slotless motors. Since there are no stator teeth, the magnetic saturation of the core is minimal, allowing for more flexibility in design. Thus, using a greater quantity of permanent magnets allows for achieving higher BEMF. As the number of poles increases, the amount of magnet used per pole decreases, resulting in a lower BEMF. Therefore, careful consideration is required when selecting

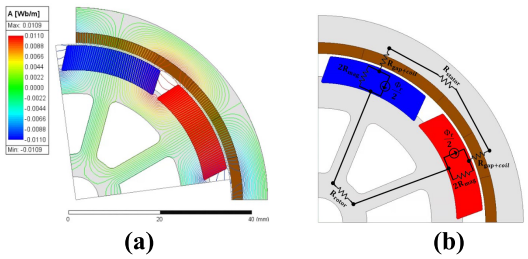

Fig. 6. (a) Slotless model magnetic flux line. (b) Slotless model magnetic equivalent circuit.

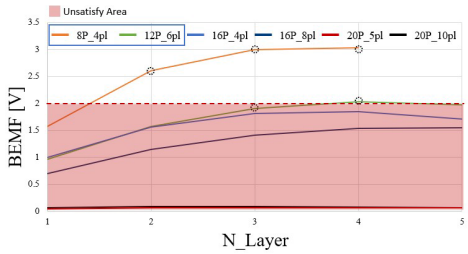

Fig. 7. Analysis of back EMF based on the number of permanent magnet poles and coil layers.

the number of poles. In addition, in slotless motors, the increase in the number of coil layers and the thickness of SPM permanent magnets lead to an increase in the magnetic airgap. An increase in the magnetic airgap results in a decrease in output. Therefore, the number of poles and coil layers must be determined considering this aspect. If the number of coil layers becomes too high, it may pose difficulties in manufacturing. However, leveraging the advantage of using numerous permanent magnets in slotless motors, a range of coil layer numbers satisfying the desired output needs to be determined.

Fig. 8(a) shows the principle of Cogging torque. The force with which the permanent magnets and the stator teeth iron core tend to adhere is known as the Cogging Torque [10], [11]. In slotless motors, the uniform reluctance difference across the stator teeth iron core eliminates Cogging Torque theoretically, resulting in Zero Cogging. Fig. 8(b) shows a graph comparing the 2-D FEA cogging torque between the conventional model and the block coil slotless model. The structure of teeth in the stator induces reluctance unevenness, resulting in cogging torque. However, the slotless motor is expected to have significantly lower cogging torque due to the uniformity in reluctance. The conventional model exhibits a cogging torque of 26.9 mNm, while the slotless model shows 2.8 mNm. This comparison was conducted through FEA analysis, revealing a reduction in cogging torque by approximately 89.6% compared to the conventional model.

Fig. 9 shows the back EMF data of the two models. The slotless motor, devoid of stator teeth, eliminates cogging torque, allowing for a reduction in significant radial force and achieving very low THD in BEMF, thereby obtaining a sinusoidal BEMF waveform. Similarly, the conventional model, with rotor skew applied, also exhibits a sinusoidal waveform in the BEMF. In the slotless model as well, a sinusoidal BEMF waveform is observed.

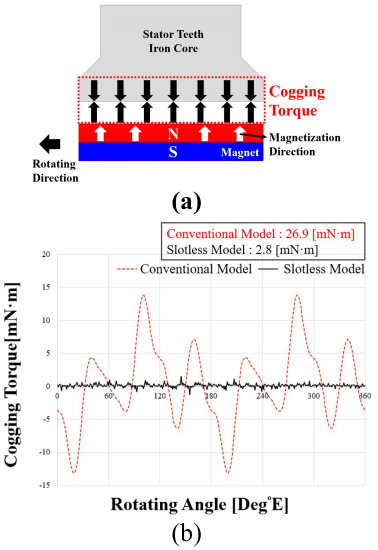

Fig. 8. Comparison of cogging torque between conventional model and block and coil slotless model. (a) Magnetic attraction between stator teeth and permanent magnet. (b) Cogging torque FEA graph.

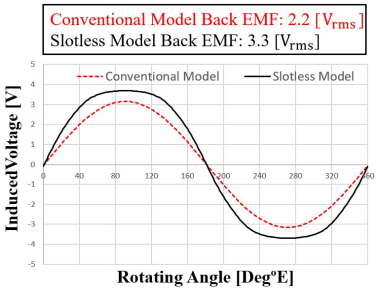

Fig. 9. Comparison of back EMF between conventional model and block and coil slotless model.

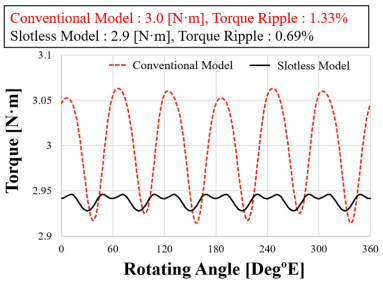

Fig. 10. Comparison of load torque between conventional model and block and coil slotless model.

Fig. 10 shows the load torque data. When analyzing the load, it is necessary to calculate the torque ripple by outputting the torque

$$T_{\text{ripple}} = \frac{T_{\text{peak\_to\_peak}}}{T_{\text{avg}}} \times 100\%. \quad (1)$$

As evident from (1) torque ripple increases as the torque amplitude increases. Slotless motors exhibit minimal variation in torque amplitude, resulting in low torque ripple. A comparison with the conventional model reveals a reduction in the torque ripple rate from 1.33% to 0.69%, approximately 48.12% lower. This reduction is attributed to the absence of stator teeth, which typically influence torque ripple.

TABLE II
TWO-DIMENSIONAL FEA DATA OF CONVENTIONAL AND SLOTLESS MODEL

PARAMETER	UNIT	CONVENTIONAL MODEL	SLOTLESS MODEL
Cogging Torque	mNm	26.9	2.8
Back EMF	Vrms	2.2	3.3
Rotating Speed	rpm	1,000	1,000
Load Torque	Nm	3	2.9
Torque ripple	%	1.33	0.69
L2L Max(+IR)	Vpeak	7.6	10.8
Current	Arms	48	30
Current Density	A/mm^2	10.4	14.9
Copper Loss	W	89.9	65.8
Core Loss	W	2.4	3.1
Output Power	W	313.4	300
Efficiency	%	77.2	81.1
Gravimetric power density	W/kg	171.5	231.4

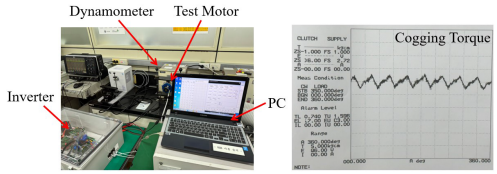

(a) (b)

Fig. 11. (a) Motor test equipment. (b) Cogging torque test.

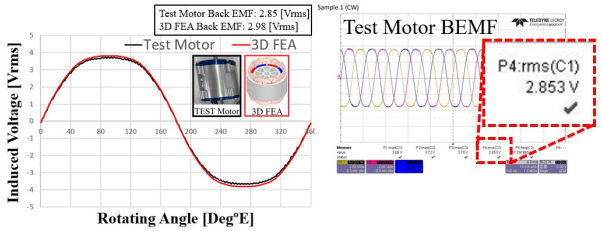

Fig. 12. Noload BEMF Test and 3-D FEA results.

Table II shows the 2-D FEA data for both the conventional model and the slotless model. It can be concluded that the slotless model significantly reduces cogging torque and torque ripple. Also, the gravimetric power density is higher in the slotless model.

IV. C-TYPE EPS SLOTLESS MOTOR TEST DATA

Fig. 11(a) shows the environment in which the test motor was measured. Fig. 11(b) shows the measured cogging torque. Slotless motor lacks stator teeth, resulting in no variation in magnetic reluctance as the rotor rotates. Therefore, the cogging torque should theoretically be zero. As demonstrated in Fig. 11(b), our experimental results confirmed that the cogging torque is indeed minimal.

Fig. 12 shows a comparison of Noload Back EMF between the test motor and the 3-D FEA simulation. The test motor recorded 2.85 V_{rms}, while the 3-D FEA yielded 2.98 V_{rms}, indicating a difference of 4.56%. During actual testing, a slight reduction in BEMF was observed, yet it remained within a satisfactory margin of error of 5%.

V. CONCLUSION

This article proposed the design of a slotless motor for C-Type EPS, replacing the conventional motor. In conventional motors with slots, the stator teeth structure necessitates consideration of magnetic saturation, which limits the amount of permanent magnets that can be used. However, slotless motors do not have stator teeth, so magnetic saturation does not occur, allowing for a greater amount of permanent magnets. Increasing the amount of permanent magnets enhances torque and enables motor miniaturization. Ultimately, an optimal design was achieved to maximize gravimetric power density. In addition, unlike conventional slotless motors that are made solely with coils, the EPS slotless motor in this article is designed using a modular assembly method with bonded coils and blocks. By designing a slotless motor, the cogging torque, which arises from the fluctuation of reluctance in the conventional model due to the presence of stator teeth, was reduced by approximately 90.54%. In addition, the torque ripple, a major cause of vibration and noise, was reduced by about 48.12%. The proposed design was validated by manufacturing and testing prototype motors, measuring parameters such as noload back EMF, cogging torque.

ACKNOWLEDGMENT

This work was supported in part by Korea Institute of Energy Technology Evaluation and Planning (KETEP) grant funded by Korean Government (Ministry of Trade, Industry and Energy, MOTIE) (20214000000060, Department of Next Generation Energy System Convergence based on Techno-Economics Platform, STEP) and in part by the Basic Research Program funded by the Korea Institute of Machinery and Materials (KIMM), grant number NK248I.

REFERENCES

[1] L. Hao, M. Lin, D. Xu, and W. Zhang, "Cogging torque reduction of axial field flux-switching permanent magnet machine by adding magnetic bridge in stator tooth," *IEEE Trans. Appl. Supercond.*, vol. 24, no. 3, pp. 1–5, Jun. 2014.

[2] W. Ren, Q. Xu, Q. Li, and L. Zhou, "Reduction of cogging torque and torque ripple in interior PM machines with asymmetrical V-type rotor design," *IEEE Trans. Magn.*, vol. 52, no. 7, pp. 1–5, Jul. 2016.

[3] Y. Ueda and H. Takahashi, "Cogging torque reduction on transverse-flux motor with multilevel skew configuration of toothed cores," *IEEE Trans. Magn.*, vol. 55, no. 7, pp. 1–5, Jul. 2019.

[4] Z. Li, X. Yu, X. Wang, and X. Xing, "Optimization and analysis of cogging torque of permanent magnet spherical motor," *IEEE Trans. Appl. Supercond.*, vol. 31, no. 8, pp. 1–5, Nov. 2021.

[5] J. Zhao, W. He, W. Fu, Y. Ding, and Y. Guo, "Comparative studies on performances of slotted and slotless high-speed PMBLDC motors," *IEEE Access*, vol. 12, pp. 13431–13441, 2024.

[6] D. Steinert, T. Nussbaumer, and J. W. Kolar, "Evaluation of one- and two-pole-pair slotless bearingless motors with toroidal windings," *IEEE Trans. Ind. Appl.*, vol. 52, no. 1, pp. 172–180, Jan. 2016.

[7] W. Cheng, G. Cao, Z. Deng, L. Xiao, and M. Li, "Analytical solution for electromagnetic torque of ultrahigh speed AFPM motor with slotless stator core and toroidal coils," *IEEE Trans. Magn.*, vol. 57, no. 2, pp. 1–5, Feb. 2021.

[8] W. Cheng, G. Cao, Z. Deng, L. Xiao, and M. Li, "Torque comparison between slotless and slotted ultra-high-speed AFPM motors using analytical method," *IEEE Trans. Magn.*, vol. 58, no. 2, pp. 1–5, Feb. 2022.

[9] Z. Yang and S. Wang, "Vibration characteristics of slotless rotating armature permanent magnet motors," *IEEE Trans. Ind. Appl.*, vol. 60, no. 1, pp. 249–255, Feb. 2024.

[10] Y.-K. Kim, S.-h. Rhyu, and I.-S. Jung, "Shape optimization for reduction the cogging torque of BLAC motor for EPS application," in *Proc. Int. Conf. Electr. Mach. Syst.*, Oct. 2010, pp. 1163–1167.

[11] L. Dosiek and P. Pillay, "Cogging torque reduction in permanent magnet machines," *IEEE Trans. Ind. Appl.*, vol. 43, no. 6, pp. 1565–1571, Nov. 2007.